https://doi.org/10.20965/jrm.2015.p0636

Paper:

Hazard Anticipatory Autonomous Braking Control System Based on 2-D Pedestrian Motion Prediction

Kazuhiro Ezawa*, **Pongsathorn Raksincharoensak****, **and Masao Nagai*****

*Department of Mechanical Systems Engineering, Faculty of Engineering, Tokyo University of Agriculture and Technology
2-24-16 Naka-cho, Koganei, Tokyo 184-8588, Japan
E-mail: 50014833002@st.tuat.ac.jp
**Department of Industrial Technology and Innovation, Faculty of Engineering, Tokyo University of Agriculture and Technology
2-24-16 Naka-cho, Koganei, Tokyo 184-8588, Japan
E-mail: pong@cc.tuat.ac.jp
***Japan Automobile Research Institute
1-1-30 Shibadaimon, Minato, Tokyo 105-0012, Japan
E-mail: mnagai@jari.or.jp

[Received June 29, 2015; accepted October 1, 2015]

This paper discusses 2-dimensional (2-D) pedestrian motion prediction and autonomous braking control for enhancing the collision avoidance performance of an active safety system. The paper targets a typical scenario involving a pedestrian walking toward a parked vehicle on a crowded urban road. The pedestrian is not expected to continue walking in a straight line. Conventional first-order motion prediction accuracy alone is not enough to predict the pedestrian motion because prediction is based on the pedestrian's current position and velocity within a finite time. We formulated a 2-D pedestrian motion model of the parked vehicle based on learning the measured trajectory of pedestrians in the same scenario. We then designed an autonomous braking control system based on whether the vehicle will overtake a pedestrian. We evaluated the validity of the proposed autonomous braking control system in simulation experiments.

Keywords: active safety, driver assistance systems, collision avoidance, autonomous braking

1. Introduction

Japanese national traffic accident statistics have shown that pedestrian have the highest number of accidents – 1,634, or 37.0% – among road fatalities. This rate is decreasing more slowly than on-board vehicle accidents, as shown in **Fig. 1** [a]. Most pedestrians – 1,310, or 83.3% – are killed when vehicles are going straight on. The main causes for drivers to trigger fatal accidents are careless driving at 35%, inattentive driving at 35% and insufficient attention to safety confirmation at 19% [1].

A number of active safety devices on the current market activate autonomous braking to avoid collisions with objects in front of them [2, 3]. In near future, it will be important to evaluate the collision avoidance performance of such systems in real-world use [4]. If pedestrians suddenly dash out into the road, current active safety systems cannot stop in time to avoid such pedestrians. Developing collision avoidance systems thus requires that pedestrian movement be made a key in achieving collision avoidance without hard braking [5–7]. Conventional pedestrian movement prediction uses first-order prediction based on the current position, direction of movement and vehicle velocity [8]. The direction in which a pedestrian is going is detected using camera images, but this does not have high resolution [9], so the detailed direction must be estimated by considering the preceding trajectory. First-order prediction is shown in **Fig. 2**, where the current direction is calculated by using Eq. (1) assuming that a pedestrian will continue going in the same direction:

$$\theta = \tan^{-1}\frac{y_{ped}(t) - y_{ped}(t-T_P)}{x_{ped}(t) - x_{ped}(t-T_P)}. \quad \quad (1)$$

Future pedestrian movement at time $(t+T_P)$ is predicted as shown in Eq. (2):

$$\begin{cases} x_{ped}(t+T_P) = x_{ped}(t) + T_P \cdot V_{ped} \cdot \cos\theta \\ y_{ped}(t+T_P) = y_{ped}(t) + T_P \cdot V_{ped} \cdot \sin\theta \end{cases} . \quad \quad (2)$$

Based on real-world urban drive data analysis, two-dimensional (2-D) pedestrian movement prediction be-

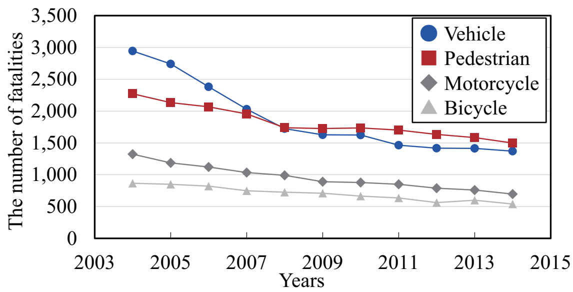

Fig. 1. Road accident statistics.

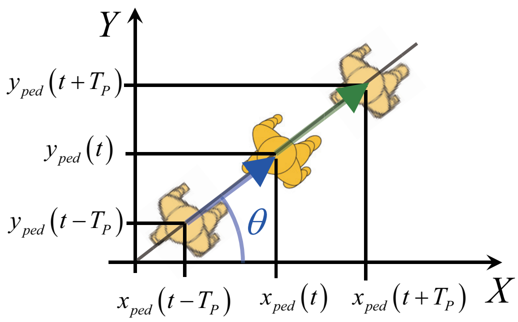

Fig. 2. First-order prediction.

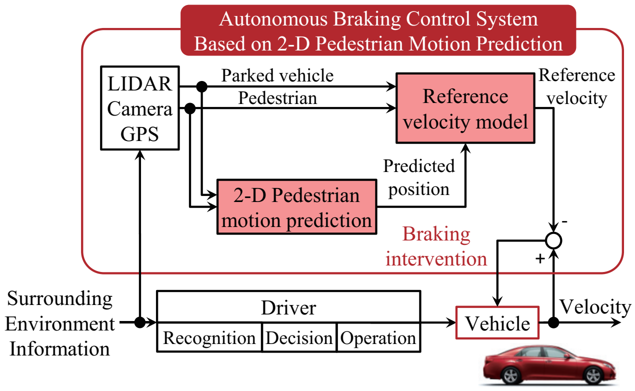

Fig. 3. Autonomous braking control system.

comes necessary in a number of situations in crowded urban areas. First-order prediction cannot, however, estimate the possibility of change in the pedestrian's direction of movement in advance.

We focused on a typical scenario in which a driver overtakes a pedestrian who walks toward a parked vehicle. In this situation, it can be predicted that the pedestrian would walk in front of a moving vehicle to avoid a parked vehicle. We discuss autonomous braking control for avoiding collisions by 2-D pedestrian movement prediction around a parked vehicle. The system is schematically diagrammed in **Fig. 3**. Section 2 shows the formulation of the pedestrian movement model at a parked vehicle based on the measured trajectory. Section 3 details the design of a reference velocity model based on the pedestrian movement model. Section 4 verifies the feasibility of the proposed system in experiments. Section 5 summarizes major conclusions obtained from our research.

2. 2-D Pedestrian Movement Model Formulation

2.1. Acquisition of Pedestrian Movement Trajectory

To clarify the characteristics of a pedestrian trajectory, we conducted experiment in data collection. Participants were instructed to walk past a parked vehicle as they usually would. As shown in **Fig. 4**, pedestrian trajectories were measured every 0.2 seconds by using a vertical LIDAR on another vehicle. Participants numbering 17 took part in experiments. Experiments used two scenarios – 2 trials walking at a normal pace and 2 walking at a quick pace.

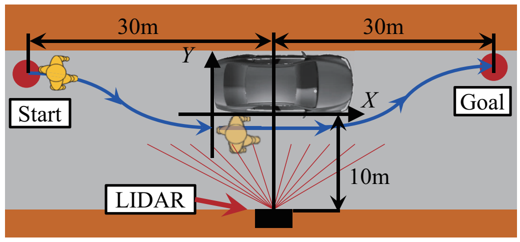

Fig. 4. Pedestrian path measurement experiments.

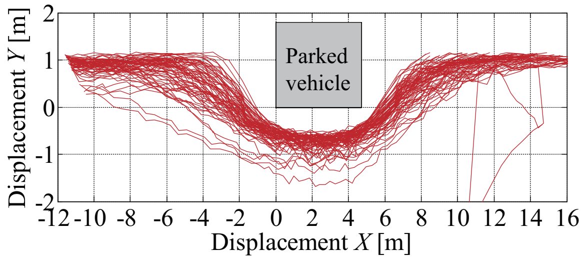

Fig. 5. Measured pedestrian trajectory.

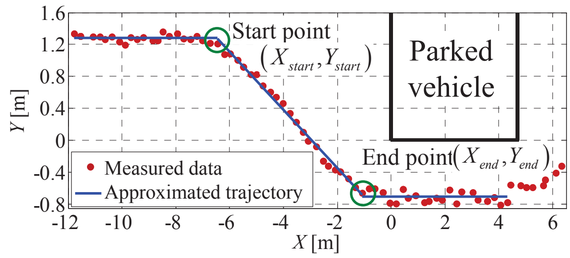

Fig. 6. Example of measured data and the approximated trajectory.

2.2. Measured-Trajectory Analysis

Measured trajectories are shown in **Fig. 5**. The X-axis shows displacement in the x-direction and the Y-axis that in the y-direction. LIDAR scans pedestrian positions as a group of dots. Because dots are influenced by arm and leg movement, it is difficult to detect the center of the pedestrian's body. To reduce the effect of movement, we calculated the pedestrian position by using the mean value of the displacement of the dots. An example of measured data and the approximated trajectory is shown in **Fig. 6**. Here, to predict pedestrian movement and avoid collisions, we must be able to predict when a pedestrian will enter the vehicle drive corridor and when a pedestrian will change direction of movement. We therefore focus on pedestrian movement until the pedestrian starts walking past the parked vehicle. As shown in **Fig. 6**, the measured trajectory is approximated by connecting straight lines.

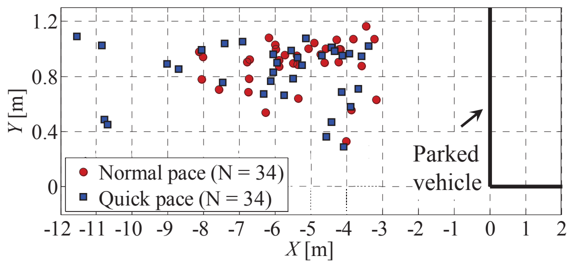

Fig. 7. Scatter plot of the lateral crossing start point.

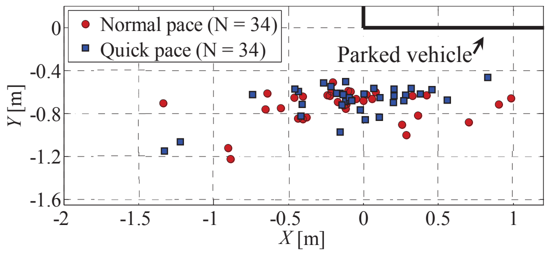

Fig. 8. Scatter plot of the lateral crossing end point.

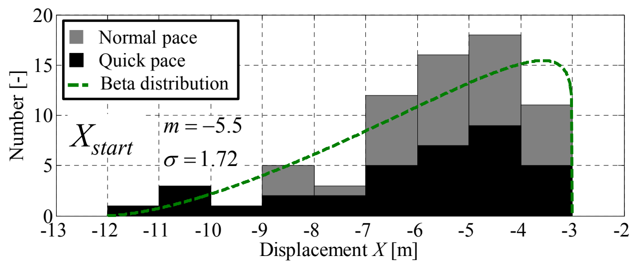

Fig. 9. Histogram of X_{start}.

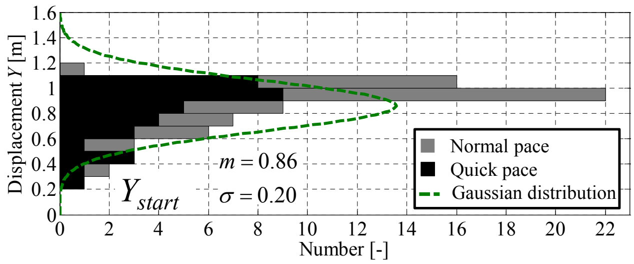

Fig. 10. Histogram of Y_{start}.

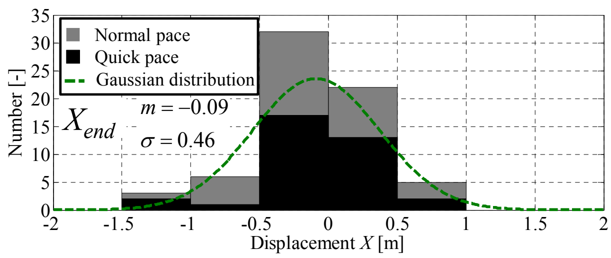

Fig. 11. Histogram of X_{end}.

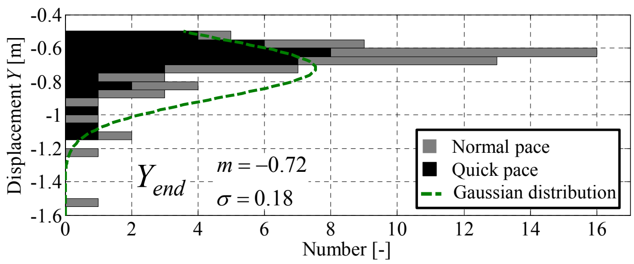

Fig. 12. Histogram of Y_{end}.

When the pedestrian is walking in the X-axis direction, the trajectory is approximated by averaging measured displacement Y. When the pedestrian walking diagonally to the X-axis, the measured trajectory is approximated by using the least squares method. Here, measured pedestrian position data is influenced by the relative position of the pedestrian's arms and legs, so the start and end points of pedestrian avoidance are judged and recorded by data analysis and start and end points are registered.

The start and end points are distributed as shown in **Figs. 7** and **8**. Note that pedestrians start avoidance before reaching position X of -3 m. Also note that pedestrians walk straight toward the right back area of the parked vehicle. Here, longitudinal and lateral start positions and longitudinal and lateral end positions of avoidance are defined as X_{start}, Y_{start}, X_{end} and Y_{end}. The distribution of X_{start}, Y_{start}, X_{end} and Y_{end} are shown in **Figs. 9–12**. The broken line in **Fig. 9** indicates a beta probability density (BPD) function. BPD function $f(x)$ is shown in Eq. (3),

$$f(x) = \frac{x^{\alpha-1}(1-x)^{\beta-1}}{B(\alpha,\beta)} \quad \ldots\ldots\ldots \quad (3)$$

$$\alpha = m\left[\frac{m(1-m)}{\sigma^2} - 1\right],$$

$$\beta = (1-m)\left[\frac{m(1-m)}{\sigma^2} - 1\right]$$

where m indicates the sample average and σ the sample's standard deviation. Variable x is limited to $0 \leq x \leq 1$ and the probability density function is calculated after the sample is normalized.

Based on data analysis, the characteristics of the measured trajectory passing the parked vehicle are as follows:

- The pedestrian walks straight toward the parked vehicle.
- To avoid having the parked vehicle block the pedestrian's way, the pedestrian changes the direction of movement based on the BPD function.
- When starting to change the direction of walking, the pedestrian walks straight toward right rear of the parked vehicle.
- Upon reaching the above area, the pedestrian changes the direction of movement again and walks beside the vehicle.

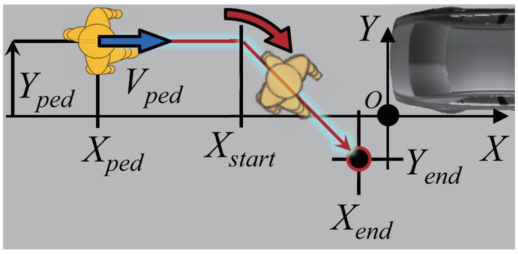

Fig. 13. Model of predicted pedestrian trajectory.

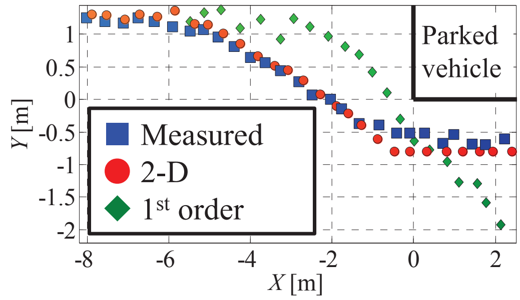

Fig. 14. Comparison of prediction of pedestrian position.

2.3. Formulation of Pedestrian Movement Prediction

The pedestrian movement prediction is formulated based on the analysis in Section 2.2.

The measured trajectory is predicted by considering current pedestrian position (X_{ped}, Y_{ped}) and the parked vehicle position shown in **Fig. 13**. The pedestrian can be predicted to walk straight toward start point (X_{start}, Y_{ped}) and then move to end point (X_{end}, Y_{end}). After arriving at the end point, the pedestrian walks beside the vehicle. Expected value X_{start} is calculated by beta distribution based on measured data.

Second, distance D_{move} [m] that the pedestrian walks in a limited time is calculated by multiplying pedestrian moving speed V_{ped} [m/s] and prediction horizon time T_P [s].

The pedestrian position is finally sequentially predicted by comparing the predicted pedestrian position and D_{move}.

2.4. Pedestrian Movement Prediction Simulation

We confirmed the validity of the proposed pedestrian movement prediction by comparing it to conventional first-order prediction. By using measured data in Section 2.1 as current position $(X_{ped}(t), Y_{ped}(t))$, predicted pedestrian position $(X_{pre}(t), Y_{pre}(t))$ at certain prediction horizon T_P was calculated.

Our research defines conventional prediction as considering only the current pedestrian moving velocity vector. The vector is calculated by considering the trajectory for a predicted horizon of 1 second, meaning that this method cannot predict whether a pedestrian will change the direction of movement.

Simulation results are shown in **Fig. 14**. The square indicates the actual position of the pedestrian directly measured. The circle indicates the pedestrian position predicted by the proposed method. The plot indicates the pedestrian position predicted by the conventional method. As shown in **Fig. 14**, the conventional method cannot predict the pedestrian position in advance. The proposed method predicts the pedestrian position beforehand by considering the parked vehicle position.

To confirm the accuracy of the proposed method, we compared actual position $(X_{ped}(t+T_P), Y_{ped}(t+T_P))$ and predicted position $(X_{pre}(t), Y_{pre}(t))$. The distance between these two points is defined as D_{error} as shown in Eq. (4):

$$D_{error}(t) = \sqrt{\left(X_{pre}(t) - X_{ped}(t+T_P)\right)^2 + \left(Y_{pre}(t) - Y_{ped}(t+T_P)\right)^2} \quad \ldots \ldots \ldots (4)$$

Here, D_{error} is evaluated from when the pedestrian begins to be detected to when the pedestrian reaches position X of +1 m. When all 68 data items have been calculated, the average of D_{error} of proposed 2-D prediction was 0.28 m, the maximum value was 1.2 m and the standard deviation was 0.18. The average of D_{error} in conventional first-order prediction was 0.44 m, the maximum value was 1.8 m and the standard deviation was 0.31 m. If the pedestrian position is predicted by using proposed 2-D prediction at a 2 second prediction horizon under the situation assumed above, 95% of error is within 0.28 ± 0.53 m. If the pedestrian position is predicted by first-order prediction under the same condition, 95% of error is within 0.44 ± 0.61 m, so the proposed 2-D prediction is superior to the conventional first-order method in this situation.

3. Autonomous Braking Control System Design

Based on the pedestrian movement prediction in the previous section, the autonomous drive system determines whether the overtake maneuver is safe. If the overtake maneuver has a certain level of risk, the ego vehicle decelerates automatically so that it follows the pedestrian.

3.1. Overtake Determination

When the vehicle approaches a pedestrian, it must remain a safe distance from the pedestrian as required by Japan's road traffic law. Here we define a lateral distance of 1.5 m as the limit. (Japan's road traffic law does not specifically define this lateral distance, but driving school instructors teach students to keep 1.5 m away.) We calculated the pedestrian position when the ego vehicle – in other words, one's own vehicle – overtakes a pedestrian as detailed below.

In the positional relation shown in **Fig. 15**, the time before the pedestrian reaches X_{start} is defined as T_{start} and

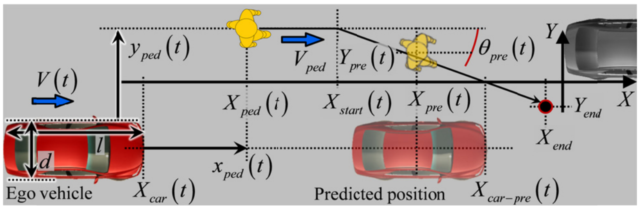

Fig. 15. Definition of the drive scenario.

the time that the ego vehicle overtakes the pedestrian is defined as T_{to}, as shown in Eqs. (5) and (6),

$$T_{start}(t) = \frac{X_{start}(t) - X_{ped}(t)}{V_{ped}(t)} \quad \dots\dots\dots \quad (5)$$

$$T_{to}(t) = T_{start}(t) + \frac{x_{ped}(t) - \left(V(t) - V_{ped}(t)\right) \cdot T_{start}(t) + l}{V(t) - V_{ped}(t) \cdot \cos\left(\theta_{pre}(t)\right)} \quad (6)$$

where l indicates the length of the ego vehicle, x_{ped} indicates the longitudinal distance to the pedestrian from the ego vehicle, $\theta_{pre}(t)$ indicates the predictive angle on changes of direction from parallel to the X-axis to the endpoint. The cosine of this angle is shown in Eq. (7).

$$\cos\left(\theta_{pre}(t)\right) = \frac{X_{end} - X_{start}}{\sqrt{\left(X_{end} - X_{start}\right)^2 + \left(Y_{pre}(t) - Y_{end}\right)^2}} \quad \dots\dots\dots \quad (7)$$

The ego vehicle overtakes the pedestrian as the pedestrian walks diagonally toward the X-axis. The predictive lateral distance to the pedestrian when the vehicle overtakes $y_{pre}(t)$ is shown in Eq. (8),

$$\begin{aligned} y_{pre}(t) &= Y_{pre}(t) - Y_{car} - \frac{d}{2} \\ &= Y_{ped}(t) - \left(T_{to} - T_{start}\right) \cdot V_{ped} \cdot \sin\left(\theta_{pre}(t)\right) \\ &\quad - Y_{car} - \frac{d}{2} \quad \dots\dots\dots \quad (8) \end{aligned}$$

where d indicates the width of the ego vehicle.

3.2. Reference Acceleration Command Calculation

We assume in this research that the pedestrian will change direction and enter the vehicle drive corridor. If a safe overtake maneuver is not possible, the autonomous braking control system produces two different decelerations based on the time before collision with the pedestrian T_{tc}. The time to collision with the pedestrian T_{tc} is shown in Eq. (9).

$$T_{tc}(t) = \frac{x_{ped}(t)}{V(t)} \quad \dots\dots\dots \quad (9)$$

If $1.4 < T_{tc} < 5$, this algorithm does not avoid collision by stopping but instead decelerates to the same speed as the pedestrian and waits for the pedestrian to pass the parked vehicle to realize natural driving behavior. Reference acceleration a_x^* is derived as shown in Eq. (10) by considering the time to terminal state T_{dec} and the distance that the pedestrian will move during T_{dec},

$$a_x^*(t) = -\frac{V(t)^2 - V_{ped}(t)^2}{2 \cdot \left(x_{ped}(t) + V_{ped}(t) \cdot T_{dec}(t) - \alpha\right)} \quad (10)$$

where α indicates the longitudinal distance margin that the ego vehicle maintains when the ego vehicle follows the pedestrian. Under the condition that the ego vehicle velocity is $V(t)$, acceleration is $a_x(t)$, pedestrian velocity $V_{ped}(t)$ and the longitudinal distance to the pedestrian is $x_{ped}(t)$ at certain time t, the distance between the ego vehicle and the pedestrian is as shown in Eq. (11):

$$\begin{aligned} &V(t) \cdot T_{dec}(t) + \frac{1}{2} \cdot a_x(t) \cdot T_{dec}(t)^2 + \alpha \\ &= V_{ped}(t) \cdot T_{dec}(t) + x_{ped}(t). \quad \dots\dots \quad (11) \end{aligned}$$

$T_{dec}(t)$ is calculated as shown in Eq. (12) by simplifying Eq. (11):

$$\begin{aligned} T_{dec}(t) = \frac{1}{a_x(t)} \Big\{ &-\left(V(t) - V_{ped}(t)\right) \\ &+ \sqrt{\left(V(t) - V_{ped}(t)\right)^2 - 2 \cdot a_x(t) \cdot \left(x_{ped}(t) - \alpha\right)} \Big\} \quad (12) \end{aligned}$$

Reference velocity V^* is calculated by integrating reference acceleration a_x^* as shown in Eq. (13):

$$V^*(t) = V_0 - \int a_x^*(t)\,dt. \quad \dots\dots\dots \quad (13)$$

The braking distance D_{stop} equation is shown in Eq. (14):

$$D_{stop} = -\frac{V^2}{2 \cdot a_x}. \quad \dots\dots\dots \quad (14)$$

We assume that the pedestrian moving velocity is 2 m/s based on average walking speed as analyzed from camera observation. We also assume that the ego vehicle is running at the same velocity 5 m behind the pedestrian. By substituting the condition determined for Eq. (14), the ego vehicle avoids collisions by using a gentle deceleration of 0.4 m/s^2 and stopping within 5 m if the pedestrian suddenly stops walking. We therefore define the value of α as 5 m.

If a safe overtake maneuver is clearly not possible at timing in which $T_{tc} < 1.4$, the system avoids collisions by braking hard, e.g., as in automatic emergency braking (AEB). AEB generates deceleration $a^*_{x\text{-AEB}}$ of 5.88 m/s^2 (= 0.6 G) with a limited jerk of 12 m/s^3 [10].

3.3. Effectiveness of Autonomous Braking Control

The effectiveness of the collision avoidance system and 2-D prediction we have proposed was verified by simulations. We compared the proposed systems in situations in which the ego vehicle tries to overtake a pedestrian walking toward a parked vehicle. Simulation conditions are shown in **Fig. 16** and **Table 1**. Simulation results are shown in **Fig. 17**, where the ego vehicle, including first-order prediction, could not estimate changes in direction before pedestrians changed direction. At timing in which

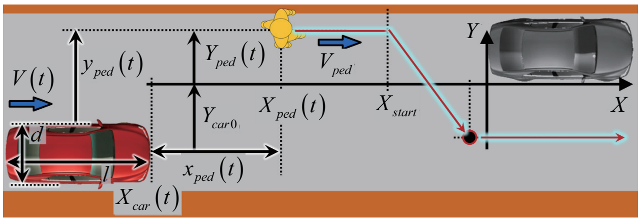

Fig. 16. Simulation and experiment conditions.

Table 1. Simulation parameters.

Definition	Symbol	Value	Unit
Initial velocity of the vehicle	V_0	24	km/h
Velocity of the pedestrian	V_{ped}	1.6	m/s
Initial X-axis vehicle position	X_{car0}	-51	m
Initial Y-axis vehicle position	Y_{car0}	-1.3	m
Initial X-axis pedestrian position	X_{ped0}	-13	m
Initial Y-axis pedestrian position	Y_{ped0}	1.2	m
X-axis direction change start position	X_{start}	-6	m
X-axis direction change end position	X_{end}	-0.5	m
Y-axis direction change end position	Y_{end}	-0.8	m

the pedestrian started to avoid the parked vehicle, time to collision with pedestrian T_{tc} is shorter than 1.4. The ego vehicle with the system including first-order prediction must therefore avoid a collision through hard braking. The ego vehicle with 2-D prediction started deceleration before a pedestrian changed its direction of movement and followed the pedestrian at a distance of 5 m. These results show that our proposed collision avoidance system effectively avoided collisions in the focused-on situation.

4. Experiments

4.1. Conditions

We confirmed the effectiveness of our proposed system in experiments under two conditions. One condition was an intentional near miss situation caused by deactivating the autonomous braking control system and the other condition was with the autonomous braking control system activated. Parameters are the same as those in **Fig. 15** and experiment parameters are shown in **Table 2**.

First, the ego vehicle and the pedestrian stop at their initial position. Next, the driver accelerates the ego vehicle to initial velocity V_0 (= 25 km/h). The pedestrian starts walking when the ego vehicle reaches experiment start position X_0 (= −55 m). The ego vehicle detects the pedestrian by using LIDAR on the front of the vehicle and predicts pedestrian movement. Last, the ego vehicle decelerates automatically based on pedestrian movement prediction by using an electric actuator attached to the brake pedal. Here, real-time longitudinal displacement of ego vehicle X_{car} is obtained by using odometry with a given initial vehicle position. Lateral vehicle displacement Y_{car} and the velocity of the pedestrian's movement are considered as constant values.

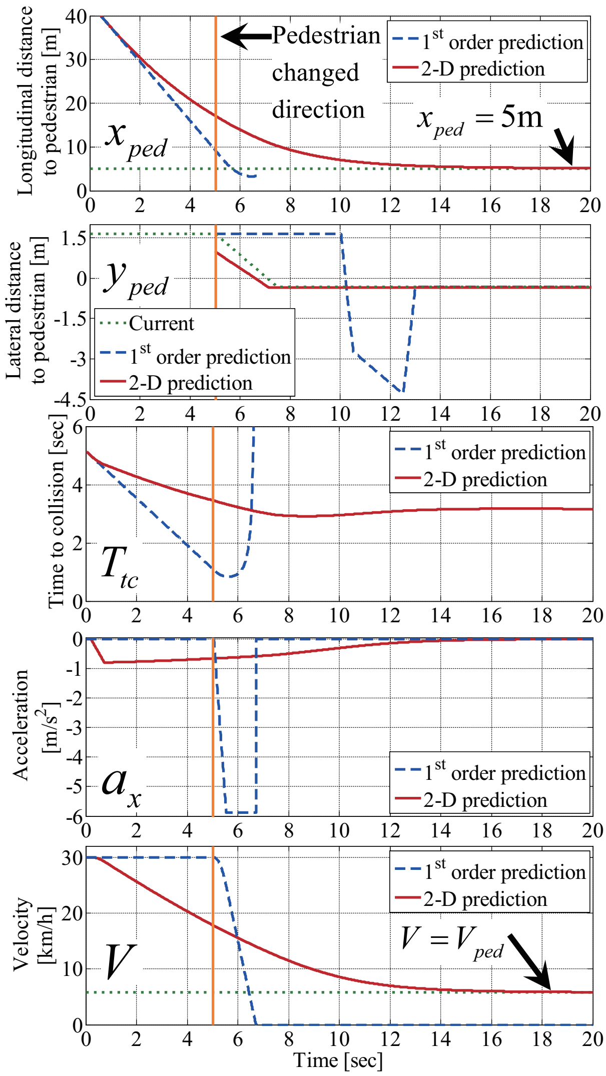

Fig. 17. Comparison of our collision avoidance system based on first-order and 2-D prediction.

Table 2. Experiment parameters.

Definition	Symbol	Value	Unit
Initial velocity of the vehicle	V_0	24	km/h
Velocity of the pedestrian	V_{ped}	1.6	m/s
Initial X-axis vehicle position	X_{car0}	-50	m
Initial Y-axis vehicle position	Y_{car0}	-2.0	m
Initial X-axis pedestrian position	X_{ped0}	-18	m
Initial Y-axis pedestrian position	Y_{ped0}	1.0	m
X-axis direction change start position	X_{start}	-6.0	m
X-axis direction change end position	X_{end}	-0.5	m
Y-axis direction change end position	Y_{end}	-0.8	m

4.2. Pedestrian Detection Using LIDAR

We detected pedestrians and predicted pedestrian movement in real time using the LIDAR. Object recognition using the LIDAR is shown in **Fig. 18**. First, objects

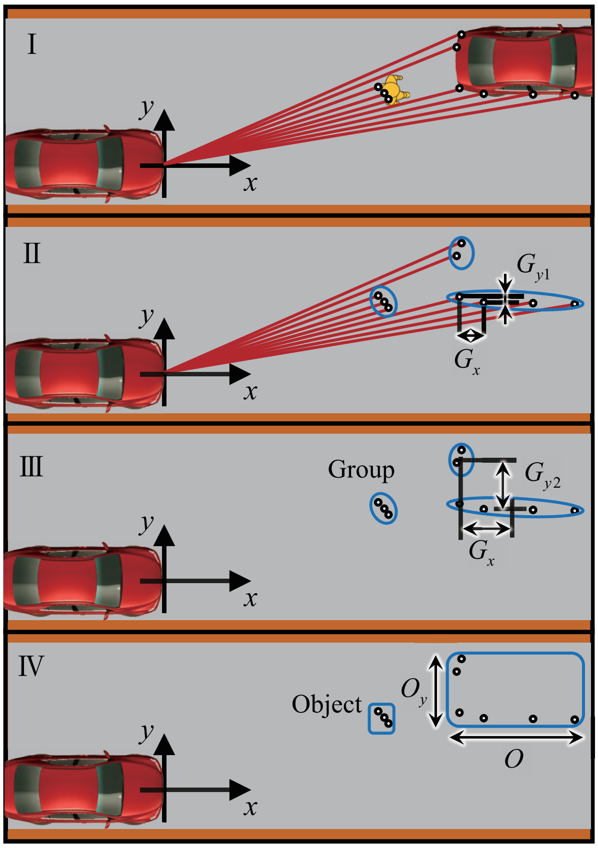

Fig. 18. Object recognition using LIDAR.

detected in the LIDAR range and FOV are shown as point clouds in I. Next, point clouds are recognized as a group if certain points next to each other are within threshold limits for data association G_{x1} and G_{y1}, as shown in II. Minimum and maximum displacement values are registered for object recognition. If these groups are recognized as objects, however, a problem arises of the parked vehicle being divided into two groups as shown in II. The small group, which is really part of the parked vehicle, could also be misdetected as a pedestrian. To solve this problem, we had groups recognized as groups if the centers of groups existed within the limits of thresholds G_{x2} and G_{y2} as shown in III. Objects are thus recognized by considering their length as shown in IV. Objects in experiments are thus recognized as pedestrians if the object is narrower than O_x [m] and O_y [m].

4.3. Autonomous Braking Pedal Control

The autonomous braking pedal control system is shown in **Figs. 19** and **20**. To follow reference acceleration and velocity without delay, we introduced lead time T_C ($=0.5$ s). The reference acceleration and velocity are calculated by considering lead time as shown in Eqs. (15) and (16):

$$a_x^*(t+T_C) = a_x^*(t) + T_C \cdot \dot{a}_x^*(t) \quad \ldots \ldots \quad (15)$$

$$V^*(t+T_C) = V^*(t) + T_C \cdot a_x^*(t) + \frac{1}{2} T_C^2 \cdot \dot{a}_x^*(t) . \quad (16)$$

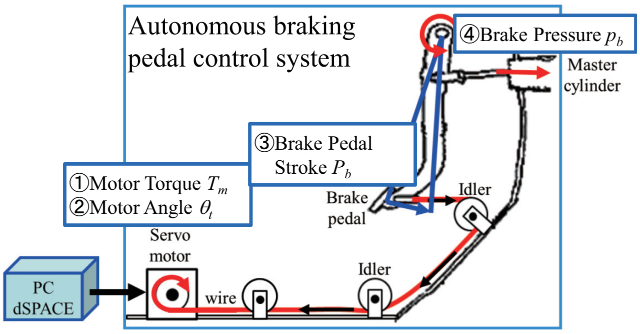

Fig. 19. Components of the autonomous braking pedal control system.

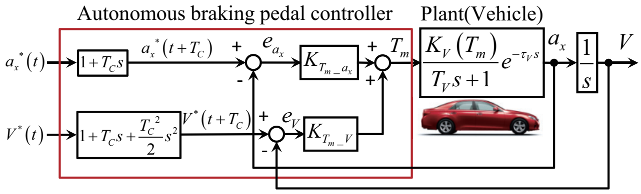

Fig. 20. Block diagram of the autonomous braking pedal control system.

Braking system control laws are shown in Eqs. (17)–(19).

$$T_m(t) = K_{T_m\_V} \cdot e_V(t) + K_{T_m\_a_x} \cdot e_{a_x}(t) \quad \ldots \quad (17)$$

$$e_V(t) = [V^*(t+T_C)] - [V(t)] \quad \ldots \ldots \quad (18)$$

$$e_{a_x}(t) = [a_x^*(t+T_C)] - [a_x(t)] \quad \ldots \ldots \quad (19)$$

Feedback variables are determined by considering final value theorems.

4.4. Experiment Results

Portions of a movie of experiments using the autonomous braking control system are shown in **Fig. 21**. Experiment results under the condition that the autonomous braking pedal control system is deactivated and activated are shown in **Figs. 22** and **23**. Note in **Fig. 22** that the ego vehicle would have collided with the pedestrian if the pedestrian has not stopped. Note in **Fig. 23** that the autonomous braking control system maintained enough margin between the vehicle and the pedestrian to keep them from colliding by decelerating based on the 2-D pedestrian movement prediction indicated by the broken line at top in **Fig. 22**. The autonomous braking pedal control system made the vehicle decelerate and traced the reference acceleration and velocity without delay, i.e., the proposed autonomous braking control system based on 2-D pedestrian movement prediction effectively enhances collision avoidance performance.

5. Conclusions

This research has detailed 2-D pedestrian movement prediction and autonomous braking control system for

Fig. 21. Experiment images.

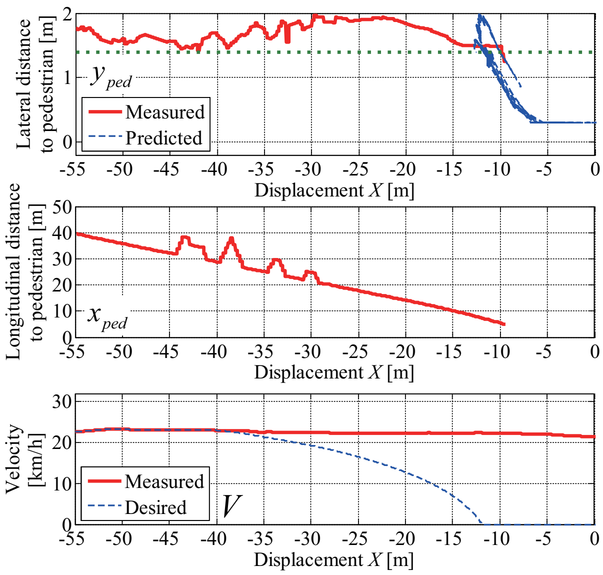

Fig. 22. Near collision situation without autonomous braking.

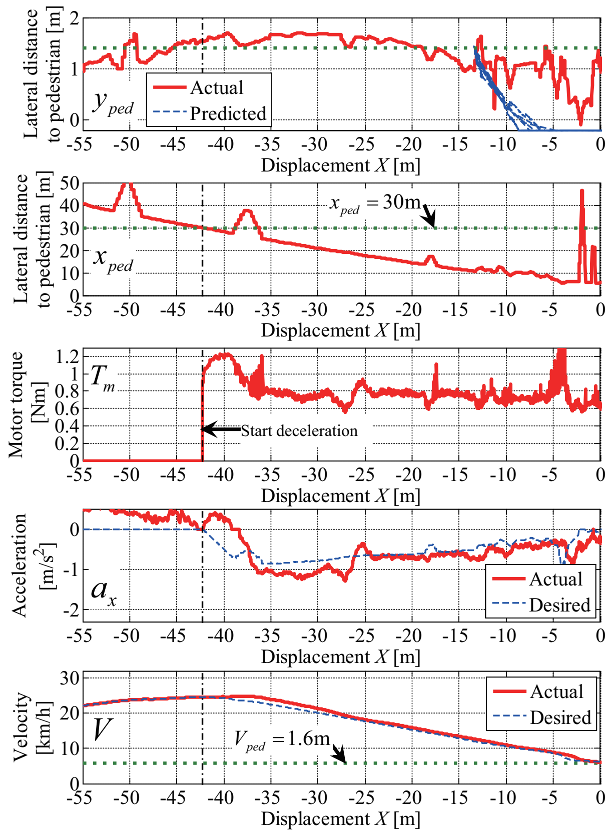

Fig. 23. Effectiveness of our proposed autonomous braking control system.

avoiding collisions with pedestrians and enhancing the collision avoidance performance of an active safety system. We first formulated a 2-D pedestrian movement prediction method related to a parked vehicle position based on measured trajectory analysis and movement modeling. We confirmed that the proposed prediction method predicted pedestrian positions well, especially when pedestrians suddenly started crossing a road laterally while walking straight. We next formulated the overtake determination method and the reference acceleration command generator based on our proposed pedestrian movement predictor. We verified the effectiveness of the autonomous braking control system we designed by conducting simulations and experiments. We thus found that the system performs in actual practice and confirmed that the proposed autonomous braking control system based on 2-D pedestrian movement prediction effectively enhanced collision avoidance performance.

References:

[1] Institute for Traffic Accident Research and Data Analysis (ITARDA), "Car-to-Pedestrian Accidents," ITARDA Information, No.83, pp. 1-12, Japan, 2010.

[2] E. Coelingh, A. Eidehall, and M. Bengtsson, "Collision Warning with Full Auto Brake and Pedestrian Detection – a practical example of Automatic Emergency Braking," Proc. of IEEE ITSC'10, pp. 155-160, 2010.

[3] S. Makabe, "Active Safety System New EyeSight Version 2," Society of Automotive Engineers of Japan, Vol.66, No.3, pp. 88-93, 2012.

[4] S. Schramm and F. Roth, "Method to Assess the Effectiveness of Active Pedestrian Protection Safety System" Proc. of ESV Conf. 2009, Paper No.09-0398, 2009.

[5] T. Shimizu, Y. Ohama, S. Nagata, and J. Sakugawa, "A Computational Framework for Estimating Collision Risk against Pedestrians," R&D Review of Toyota CRDL, Vol.43, No.1, pp. 33-42, 2012.

[6] H. Tsuyuki, R. Hayashi, and M. Nagai, "Development of Hazard-Anticipative Driving Assistance System at Overtaking a Pedestrian on Narrow Roads," Proc. of 2013 JSAE Annual Congress (Autumn), No.125-13, pp. 5-8, 2013.

[7] R. Matsumi, R. Pongsathorn, and M. Nagai, "Study on Autonomous Intelligent Drive System Based on Potential Field with Hazard Anticipation," J. of Robotics and Mechatronics, Vol.27, No.1, pp. 5-11, 2015.

[8] N. Tiemann et al., "Predictive Pedestrian Protection – Situation Analysis with a Pedestrian Motion Model," Proc. of AVEC'10, UK, 2010.

[9] X. Cao, H. Qiao, and J. Keane, "A Low-Cost Pedestrian-Detection System with a Single Optical Camera," IEEE Trans. on Intelligent Transportation Systems, Vol.9, No.1, pp. 58-67, 2008.

[10] M. Nagai, P. Raksinsharoensak, R. Hayashi, and Y. Ishizaki, "Study on Evaluation Method for Pedestrian/Bicycle Accident Avoidance System Based on Analysis of Near-miss Incident Database," Proc. of 54th JACC, CD-ROM, pp. 222-226, 2011.

Supporting Online Materials:

[a] National Police Agency of Japan, "Annual report of the characteristics of fatal traffic accidents and status of the violation of the road traffic law enforcement during the year of 2014," 2015. http://www.e-stat.go.jp/SG1/estat/Pdfdl.do?sinfid=000028474471 [Accessed June 15, 2015]

Name:
Kazuhiro Ezawa

Affiliation:
Graduate Student, Tokyo University of Agriculture and Technology

Address:
2-24-16 Naka-cho, Koganei, Tokyo 184-8588, Japan

Brief Biographical History:
2008-2012 Bachelor degree Student, Faculty of Engineering, Tokyo University of Agriculture and Technology
2012-2014 Master Course, Graduate School of Engineering, Tokyo University of Agriculture and Technology
2014- Doctor Course, Graduate School of Engineering, Tokyo University of Agriculture and Technology

Main Works:
- "Automatic Braking Control Intervention Based on Hazard-Anticipatory Driving Characteristics in Unsignalized Intersections," Proc. of JSAE Annual Congress, Yokohama, No.465-20135256, May 2013.
- "2-D Pedestrian Motion Prediction Modeling in Urban Driving Scenario Based on Potential Field," Proc. of FAST-zero2015, pp. 39-44.

Membership in Academic Societies:
- The Society of Automotive Engineers of Japan (JSAE)

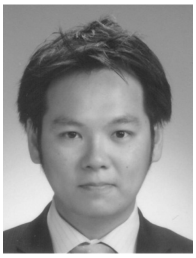

Name:
Pongsathorn Raksincharoensak

Affiliation:
Associate Professor, Tokyo University of Agriculture and Technology

Address:
2-24-16 Naka-cho, Koganei, Tokyo 184-8588, Japan

Brief Biographical History:
2004-2006 Research Associate, Tokyo University of Agriculture and Technology
2006-2011 Associate Professor (tenure track), Tokyo University of Agriculture and Technology
2011- Associate Professor (tenure), Tokyo University of Agriculture and Technology

Main Works:
- "Development of Autonomous Intelligent Driving System to Enhance Safe and Secured Traffic Society for Elderly Drivers," J. of Robotics and Mechatronics, Vol.25, No.6, pp. 966-972, 2013.
- "Driver Speed Control Modeling for Predictive Braking Assistance System Based on Risk Potential in Intersections," J. of Robotics and Mechatronics, Vol.26, No.5, pp. 628-637, 2014.

Membership in Academic Societies:
- The Japan Society of Mechanical Engineers (JSME)
- The Society of Automotive Engineers of Japan (JSAE)
- The Society of Instrumentation and Control Engineers (SICE)

Name:
Masao Nagai

Affiliation:
President, Japan Automobile Research Institute

Address:
1-11-30 Shibadaimon, Minatoku, Tokyo 105-0012, Japan

Brief Biographical History:
1977- Lecturer, Tokyo University of Agriculture and Technology
1980- Assistant Professor, Tokyo University of Agriculture and Technology
1982-1983 Visiting Researcher, Technical University of Braunschweig, Germany
1989-2013 Professor, Tokyo University of Agriculture and Technology
2013- President, Japan Automobile Research Institute

Main Works:
- P. Raksincharoensak, L. Wan, and M. Nagai, "Study on a Longitudinal Control and Guidance System for Lane Change Assistance," Int. J. of Vehicle Safety, Vol.7, No.1, pp. 37-53, 2014.

Membership in Academic Societies:
- The Japan Society of Mechanical Engineers (JSME)
- The Society of Automotive Engineers of Japan (JSAE)
- The Society of Instrumentation and Control Engineers (SICE)